Microwave assisted chloride leaching of zinc plant residues

Thomas Abo Atia[a,b*](Abo Atia is the entire surname), Jeroen Spooren[a]

[a] *Waste Recycling Technologies, Flemish Institute for Technological Research, VITO N.V.,*

Boeretang 200, 2400 Mol, Belgium

[b] SIM vzw, Technologiepark 48, 9052 Zwijnaarde, Belgium

*Corresponding author: Abo Atia Thomas, email: thomas.aboatia@vito.be, phone: +3214335177, VITO NV, Boeretang 200, Mol, Belgium

Abstract

Microwave (MW) assisted chloride leaching was studied to remove valuable and heavy metals from two zinc plant residues, *i.e.* goethite sludge and Zn-leach product.

For both materials, NaCl leaching parameters, such as temperature, NaCl concentration, leaching time and addition of acid, were optimized. For goethite sludge, the best efficiencies for Cu (45-47%), Pb (83-90%), and Zn (47-58%) extraction, with a minimal dissolution of matrix elements, were obtained at 200 °C, 300 g/L NaCl and L/S 10. At short leaching times (5 min) the maximal leachability of Cu and Zn was reached, while at longer leaching time (60 min) the Pb extraction increased to 90±1%. Zn leaching was limited due to the presence of stable franklinite ($ZnFe_2O_4$).

NaCl (280 g/L) leaching of Zn-leach product required the addition of 1 M HCl to improve metal leaching to Ag 52±3%, Bi 83±1%, Cd 82±4%, Sb 39±1%, Zn 71±2% at 200 °C, L/S 10 for 30 min. Consequently, matrix dissolution was enhanced. Metal associations in Zn-leach product were statistically investigated. The environmental impact of the MW leached materials was evaluated by a one stage leaching test, which showed a significant overall reduction in heavy metal leachability compared to untreated materials.

1. Introduction

After years of uptime, several metalliferous mining and refining facilities might cope with reduced availability for on-site disposal (*e.g.* backfilling, ponds) of process waste and by-products. Short- and long-term risks are associated to on-site waste dumping [1], such as dam failures [2].

Timely solutions are needed for re-thinking the destiny of metallurgical by-products [3] toward a sustainable exploitation of mining resources, ensuring the growing demand of today's society for raw materials, *e.g.* metals [4], and decreasing societal distrust and downsides related to mining activities worldwide. On the other hand, economic and technological challenges exist. Post-processing materials mostly contain low concentrations of valuables, which are often diluted in complex mineralogical matrices. This makes an economically viable process, for either the recovery of valuables and/or the decontamination from hazardous elements, a daunting task.

45   Both aspects of recovery and decontamination may be highly desired from industrial point of view, in

46   order to reduce wastes; decrease the hazard of the waste stream [5]; and create potential profit out of

47   metal recovery and avoidance of landfill tax.

48   The hydrometallurgical process for refining zinc relies on roasting, leaching and electrowinning of

49   concentrated zinc ore (50-60% Zn), which is the predominant used route worldwide [6]. Herein, the

50   sulfidic ore is first oxidized to zincite, ZnO, then the resulting material ''calcine'' is leached with

51   sulfuric acid to solubilize zinc as sulfate, $ZnSO_4$. After purification of Zn-pregnant solution from

52   interfering ions (*e.g.* Co, Cd and Fe), zinc is obtained in metallic form by electrowinning. Three different

53   iron removal processes exist, namely the goethite, jarosite and hematite processes [7].

54   This case study included two zinc plant residues from the goethite process. One was the insoluble

55   residue from the sulfuric acid leaching stages of calcine, named Zn-leach residue. This material is

56   generally sent to smelting industries for further processing, due to the high content of Pb - mainly

57   present as $PbSO_4$[8]- and Ag. However, penalties are applied for contaminants, such as As, Sb and Cd,

58   that influence the selling value. While, the second studied residue was goethite sludge, which is a by-

59   product of the purification of Zn-pregnant solution from solubilized iron. In this purification process,

60   iron (III) is first reduced to ferrous iron (II) with the zinc concentrate. This step enables the removal of

61   sulfur by precipitation in elemental form. Subsequently, iron (II) is re-oxidised to iron (III) with air and

62   a neutralizing agent (*e.g.* calcine) at a pH of about 2.5 [7] so that it precipitates in the form of goethite.

63   This solid is an iron oxyhydroxide of chemical structure FeOOH, from which the process name is

64   derived. The precipitation reaction can be described as follows in eq. (1).

65   (1) $2FeSO_4(l)+ 2ZnO(s)+ 1/2\ O_2(g)+ H_2O \rightleftharpoons 2FeOOH(s)+ 2ZnSO_4(l)$.
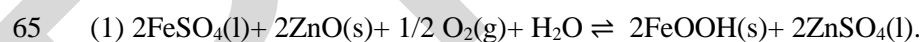
66   Goethite sludge is classified as hazardous waste, due to its considerable load of heavy metals, *e.g.* Pb,

67   Cd, Zn, As, etc. [9], and is of primary concern due to its current storage in ponds.

68   In the zinc industry, the virtuous approach to find novel solutions to treat secondary streams has already

69   started in the last decades, aiming for recovering base, *e.g.* Zn, Pb [10], and niche, *e.g.* In, Ge, Ga

70   [11,12], metals and evolving towards a near-zero-waste process concept [13].

71   High temperature processes, such as smelting, plasma fuming [14], carbothermal reduction [15], and

72   sulfating roasting followed by water leaching [16,17] were applied for zinc plant residues valorization.

73 Furthermore, extensive literature on leaching and advanced leaching (including microwave (MW)

74 assisted leaching) approaches to recover, *e.g.* Zn, Pb, Cd, and Ag, from mineral waste materials exists

75 [6,18,27–30,19–26].

76 For instance, Raghavan *et al.* performed brine leaching experiments with NaCl 100-300 g/L at pH of

77 1.5-2 for 30 min at 80-85 °C on a Ag-concentrate leach residue (Ag 0.2-03 wt%.; Pb 6-9 wt%.; Zn 32-

78 40 wt%), obtained after flotation and sulfuric acid leaching, and managed to remove up to 90-93% and

79 75-85% of Ag and Pb, respectively [19]. Preferably, Pb was then recovered by cementation with

80 metallic Al. Additionally, a recent work by Xie *et al.* showed that about 86% of Pb was leached from

81 the leach residue of Zn hydrometallurgical refining by a two-step leaching process with $CaCl_2$ ([$CaCl_2$]

82 = 3.15 M, 45 °C, 120 min, pH = 2) [31].

83 Further studies showed that leaching in chloride-bearing lixiviants promote selective solubilization of

84 elements, such as Zn, Pb, Cd, Sb, Bi [20,32,33], which are contained also in zinc plant residues. Besides,

85 it is established knowledge that the application of microwaves to a leaching system enables fast,

86 selective and homogeneous heating and thus improves leaching kinetics and selectivity [34–37].

87 The use of microwave assisted chloride leaching instead was never tested on Zn-leaching product and

88 goethite sludge.

89 Thus, in this work the benefits of microwave assisted leaching and chloride complexation chemistry

90 were coupled, whereby NaCl was used as cheap reagent for the two abovementioned zinc plant residues.

91 Both materials have distinct chemical and mineralogical compositions. For goethite sludge microwave

92 assisted NaCl leaching was studied, aiming at leaching heavy metal contaminants, *i.e.* Pb, Zn and Cu,

93 selectively from the iron- and calcium-bearing matrix. For this system the effects of temperature, time

94 and NaCl concentration were studied. While, for the Zn-leach product microwave assisted NaCl

95 leaching with and without HCl addition was investigated to extract Ag, Sb, Bi, Zn and Pb. The HCl

96 addition and leaching temperature were optimized to improve the leaching efficiency and selectivity

97 toward the target metals. The environmental quality of the materials before and after leaching was

98 evaluated.

2. Experimental

2.1 Materials

The two residues from industrial refining of zinc were provided by Nyrstar (Belgium). Both the goethite sludge and the Zn-leach product were dried until constant mass at 40 °C before the experiments. The materials had a moisture content of 34 wt% and 38 wt%, respectively.

For microwave leaching experiments, NaCl ($\geq$ 99.5 %, *Merck*) and HCl (fuming, 37%, *Merck*) solutions were used as leaching agents. MilliQ water was employed for solutions preparation, recovery/washing of residues and dilutions before ICP-OES analysis in 5% HNO_3 (67-69%, *Merck, Optima*).

2.2 Characterization of zinc plant residues

The chemical characterization of the dried residues was performed by microwave digestion according to a modified EN 13656 procedure, whereby HF was substituted by HBF_4, and the obtained digestates were analyzed with ICP-OES (*Perkin Elmer, Optima 3000 DV*). The solids were also analyzed by XRF *(Niton XL3t GOLDD+)* and XRD (*PANalytical EMPYREAN, Co radiation, BBHD,* 3D detector *PIXcel 3D)* using High-score plus software for phase identification and Rietveld quantification. TiO_2 was used as an external standard.

In addition, SEM (*FEI NOVA NANOSEM 450*) and EDX (*BRUKER QUANTAX 200* with SDD detector) analyses provided morphological, elemental and mineralogical information of solid samples that were dispersed in a resin and polished and/or Pt-coated.

Dielectric properties of the two zinc plant residues were measured by a Portable Dielectric Measurement Kit (*Püschner gmbh*) equipped with an open coaxial probe operating at a frequency of 2.45 GHz at 25 °C.

2.3 Microwave leaching

The microwave (MW) leaching experiments were performed in a *Milestone FlexiWave* laboratory microwave oven equipped with pressure-sealed Teflon reactors, withstanding high pressure (100 bar) and temperature (250 °C). For each MW treatment up to 15 reactors were placed in a carrousel that was

124   positioned in the microwave. The temperature was measured by a single optic fiber inserted in one of

125   the vessels. For this reason, in one run the experimental conditions in the reactors needs to be similar,

126   to assure a similar microwave absorption and thus temperature in the reactors. Thus, only replicate

127   experiments were performed in the same run.

128   After cooling of the reactors, the leachates were separated by vacuum filtration from the solid residues.

129   Residues were then dried at 50 °C and subsequently XRD and XRF measurements were performed.

130   The leachates were analyzed with ICP-OES (*Perkin Elmer, AVIO 500)*.

131   The leaching efficiencies for each metal were determined by the ratio of amount of metals analysed in

132   the leachate volume and the amount of metals in the starting material, as follows:

133
$$Leaching\ efficiency\ (\%) = \frac{mass\ of\ metal\ solubilized}{mass\ of\ metal\ in\ the\ starting\ material}\ x\ 100$$

134   All MW leaching conditions and parameters were tested at least in duplicate experiments (N≥ 2).

2.3.1 Microwave NaCl leaching of goethite

136   The effect of temperature (50, 100, 150, 200 °C) in 300 g/L NaCl for 30 min, time (5-min ramp and 5,

137   15, 30, 60 min dwell time) in 300 g/L NaCl at 200 °C and NaCl concentration (0, 50, 100, 200, 300

138   g/L) at 200 °C for 30 min were evaluated for MW leaching of the goethite sample, using a liquid-to-

139   solid (L/S) ratio of 10. The experiments were performed in quadruplicate (N=4) in 2 different MW

140   runs.

2.3.2 Microwave NaCl and NaCl-HCl leaching of Zn-leach product

142   Three main lixiviant compositions have been studied for the Zn-leach product: 280 g/L NaCl, HCl 0.1M

143   + NaCl 280 g/L, HCl 1M + NaCl 220 g/L. The effect of temperature (50, 100, 200 °C) was tested for

144   these three systems, keeping fixed the MW program composed of 5 min ramping to the set temperature

145   and 30 min holding time. Room temperature leaching experiments were also performed in a

146   thermostatic water bath at 25 °C for comparison. All the experiments were performed at L/S=10.

147   The statistical analysis for metal leachability correlation of the Zn-leach product was performed on the

148   obtained experimental dataset for replicated experiments (N=4) by OriginPro 2019 (v. 9.6) software.

149   The statistics were refined by a Spearman's rank-order correlation, given the non-normal distribution

150   of the leaching efficiencies [51]. This analysis allowed to thoroughly investigate metal correlations and

151   mineralogical association in Zn-leach product.

2.4 One stage leaching test

153   The starting materials and obtained residues after microwave leaching of goethite and Zn-leach product,

154   using NaCl 300 g/L and HCl 0.1 M + NaCl 280 g/L, respectively, at 200 °C for 30 min, underwent a

155   one stage batch leaching test to evaluate their environmental performance. The test is performed

156   according to the Flemish (Belgium) standard CMA/2/II/A.12 [38] that is based on the European

157   standard test method EN 12457-4:2002 [39]. In the case of the starting material the exact procedure, as

158   described in the standard, was followed. Whereas for the leach residues, the minimum required amount

159   of material (*i.e.* 90 g of dry material) was not available and the test was therefore downscaled to

160   accommodate for leaching of the material in milliQ water at a liquid to solid ratio of 10 for 24 h in an

161   overhead shaker. The leaching trend of the one stage batch leaching test correlates to that of the standard

162   column leaching test [40,41]. Thus, the one stage batch leaching test can be used as a fast leaching test

163   for the screening of leachabilities of aggregate materials.

3. Results and discussion

3.1 Characterization of goethite sludge and Zn-leach product

166   The zinc plant residues investigated in this work exhibited a complex mineralogy and chemical

167   composition. The dried goethite sludge was an iron-rich material (24%), and unlike the name may

168   suggest, the goethite (FeOOH) phase was not detected by XRD analysis (Figure S1), However, a

169   significant presence of amorphous material (63%) was observed and the background humps coincide

170   with the patterns of iron oxide phases. Gypsum, $CaSO_4 \cdot 2H_2O$ (15-16%), franklinite, $ZnFe_2O4$ (10%),

171   jarosite, $KFe_3(SO_4)_2(OH)_6$ (10%), and other minor mineral phases *e.g.* SiO_2, $Ca(OH)_2$, $ZnSiO_4$ also

172   occurred in the dried material. The chemical characterization of goethite sludge indicated that the main

173   valuable and/or polluting elements of the goethite sludge were As, Cd, Cu, Pb, and Zn (Table 1).

174   SEM/EDX analyses (Figure S2) provided significant information about the chemical and mineralogical

175 association of Zn and Pb. Aside from observable franklinite and $ZnSiO_4$ minerals, a diffused EDX signal

176 was seen for Zn in the iron-rich phases, which can be associated to its presence as adsorbed metal ion

177 or salt (*i.e.* $ZnSO_4$ from sulfuric leaching stages). Furthermore, Zn was present in combination with K,

178 Fe, S, O, and Pb, showing a likely association to jarosite. Pb was presumably included in jarosite and

179 in dispersed $PbSO_4$ particles (Figure S3).

180 *Table 1: Elemental characterization of goethite sludge and Zn-leach product.*

wt%	Goethite sludge	Zn-leach product
Ag	<LOD	0.101 ± 0.007
As	0.35 ± 0.5	0.89 ± 0.03
Bi	<LOD	0.110 ± 0.001
Ca	5.5 ± 0.1	7.5 ± 0.9
Cd	0.049 ± 0.007	0.20 ± 0.02
Cu	0.40 ± 0.02	0.21 ± 0.02
Fe	24.1 ± 0.6	3.62 ± 0.02
Pb	1.8 ± 0.1	14 ± 1
Si	1.27 ± 0.05	7.4 ± 0.2
Sb	0.047 ± 0.007	0.19 ± 0.02
Zn	5.80 ± 0.07	3.5 ± 0.3

181

182 With regard to the Zn-leach product, the identified mineral phases were gypsum, $CaSO_4 \cdot 2H_2O$ (30-

183 40%), anglesite, $PbSO_4$ (20-30%), plumbojarosite, $(Pb_{0.34}K_{0.19})Fe_3(SO_4)_2(OH)_6$ (15-18%), elemental

184 sulfur, S (7-9%), sphalerite, ZnS ($\approx$1-3%), gunningite, $ZnSO_4 \cdot H_2O$ (1-4%), and quartz, SiO_2 (7-10)%

185 (SI, Figure S4). SEM/EDX characterization highlighted a potential association of Bi with Pb, in S and

186 O rich particles, likely as $PbSO_4$. A diffused Bi signal was also observed from different areas of the

187 sample (Figure S5). Due to the low concentrations of Ag, Cd, Cu, Sb in Zn-leach product, the mineral

188 phases including these elements were not identified. The elemental characterization (Table 1) showed

189 that, in addition to Pb and Zn, the recovery of Ag, Bi, Cu, and Sb (0.1, 0.1, 0.2 and 0.2 wt%,

190 respectively) could be relevant for process applicability.
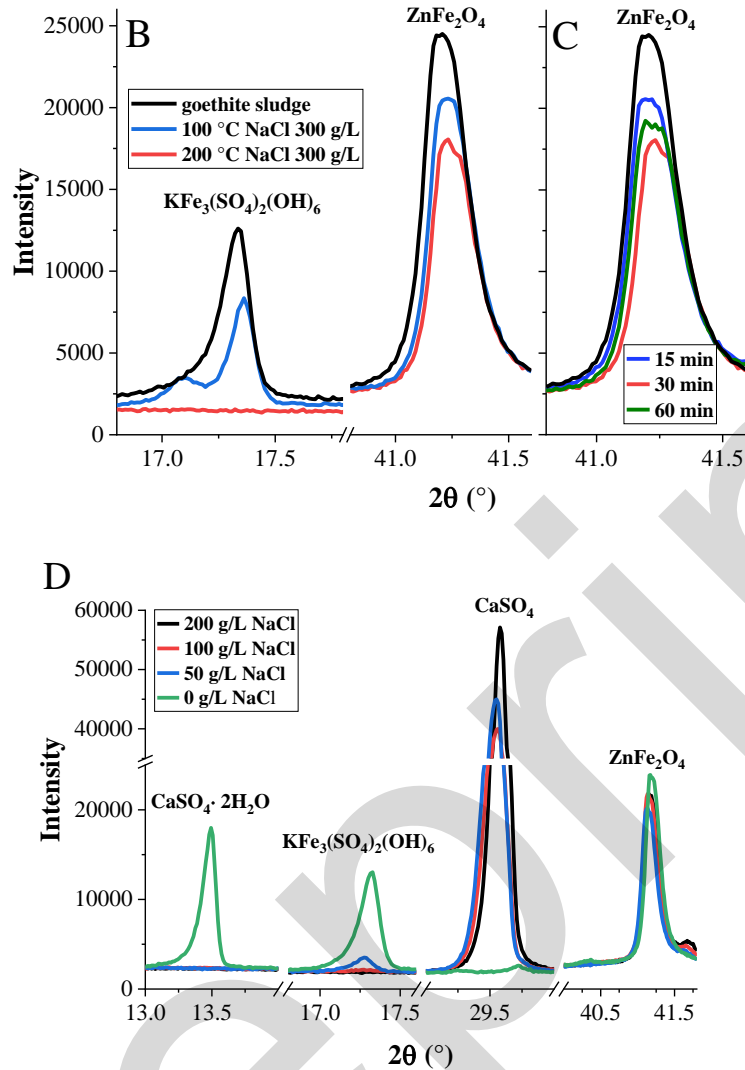
191 **3.2 Goethite sludge**

192 The effects of NaCl concentration (A), temperature (B) and leaching time (C) during microwave

193 assisted NaCl leaching of goethite sludge on metal leachabilities and mineralogy of the solid leach

194 residues are presented Figure 1 and Figure 2, respectively. The obtained results provide an insight into

195 the leaching behavior of the matrix elements, Fe and Ca, and the elements of interest to be recovered,

196 Cd, Cu, Pb and Zn, in the studied leaching system and will allow for its optimization.
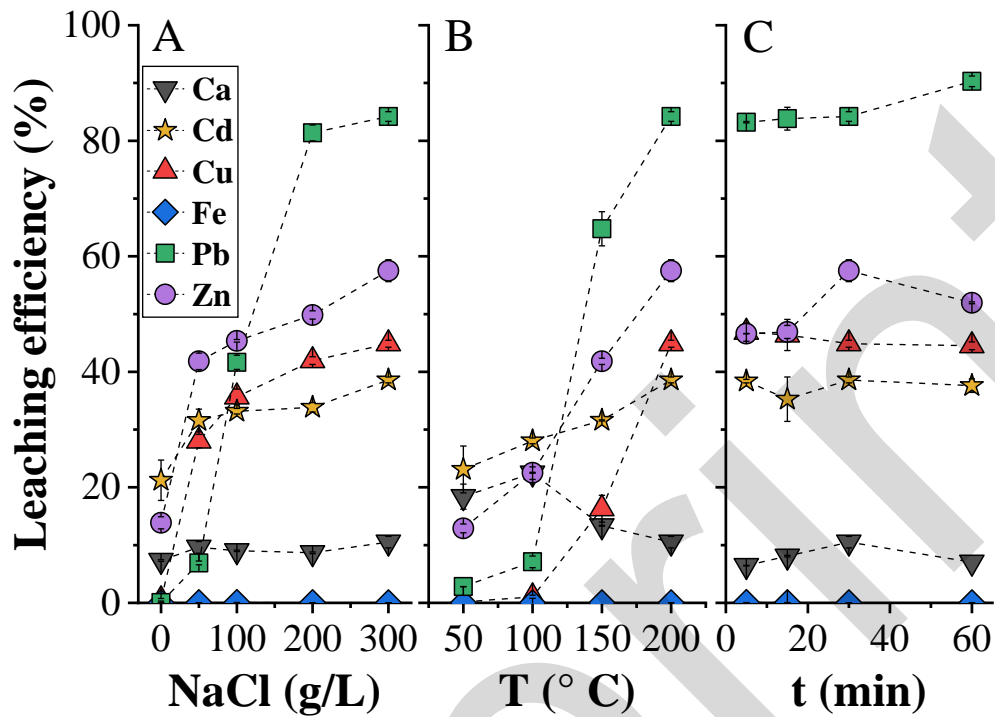
197

198 *Figure 1: Leaching efficiency after MW leaching for Ca, Cd, Cu, Fe, Pb, and Zn from goethite sludge*
199 *vs (A) NaCl concentration (0, 50, 100, 200, 300 g/L) at 200 °C for 5+30 min, (B) temperature (50, 100,*
200 *150, 200 °C) with NaCl 300 g/L for 5+30 min , and (C) time (5-min ramp + 5, 15, 30, 60 min) at 200°C*
201 *with with NaCl 300 g/L. Dotted lines are shown as a guide for the eye.*

202
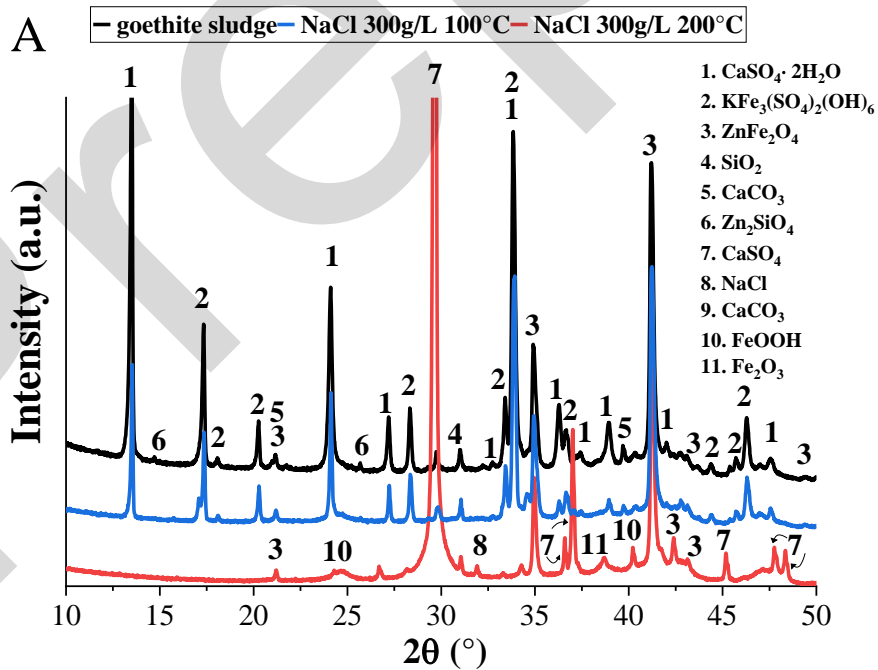
203
204

205

206 *Figure 2: XRD patterns of goethite sludge and goethite sludge after MW leaching with NaCl 300 g/L,*
207 *5+30 min, at 100 and 200 °C (A). Effect of temperature for MW leaching with NaCl 300 g/L, 5+30 min*
208 *(100- 200 °C) on jarosite, $KFe_3(SO_4)_2(OH)_6$, and franklinite, $ZnFe_2O_4$, peaks (B). Effect of leaching*
209 *time (5+15, 30, 60 min) on franklinite, $ZnFe_2O_4$, with NaCl 300 g/L, at 200 °C (C). Effect of NaCl*
210 *concentration (0-200 g/L) on jarosite, $KFe_3(SO_4)_2(OH)_6$, and $CaSO_4$ mineral phases after MW leaching*
211 *at 200 °C, for 5+30 min (D).*

212

213 For a further understanding of the speciation of elements in goethite sludge, MW leaching at 200 °C for

214 30 min in DI water was performed (Figure 1A). A modest leaching of Zn (14±1%) and Cd (21±4%)
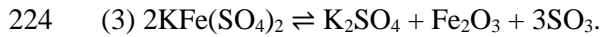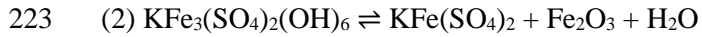
215 indicated that a fraction of both elements occurred as absorbed ions and/or soluble sulfates. Whereas,

216 the negligible Pb extraction (0.04%) agreed with the low solubility of anglesite and jarosite in water

217 and low Cu leaching (0.5±0.2%) suggested their occurrence in scarcely soluble mineral phases.

218 At all tested conditions, the Fe dissolution from goethite sludge was very low (<0.06%). This

219 observation can be associated to the thermodynamic stability of iron as hematite (Figure S6), goethite,

220   chloride substituted iron hydroxides *e.g.* $Fe(OH)_{2.7}Cl_{0.3}$, and/or amorphous solid Fe-containing phases

221   [43]. It was observed that jarosite progressively decomposed from 0 to 200 °C (Figure 2A, B) according

222   to eq. 2, 3 [44].

223   (2) $KFe_3(SO_4)_2(OH)_6 \rightleftharpoons KFe(SO_4)_2 + Fe_2O_3 + H_2O$

224   (3) $2KFe(SO_4)_2 \rightleftharpoons K_2SO_4 + Fe_2O_3 + 3SO_3$.

225   Such thermal decomposition was supported by the appearance of crystalline hematite and goethite

226   phases in the solid residues at 200 °C, while jarosite almost completely disappeared and potassium

227   concentration levels in the leachate increased.

228   Nevertheless, a slightly increased Fe solubility (3000-18000 ppb) was observed for applied NaCl

229   concentrations in the range of 50-200 g/L at 200 °C for 30 min and could be directly related to the

230   measured pH and ORP values of the obtained leachates. At the end of the MW leaching experiments

231   the pH of the leachates at 50, 100, 200, and 300 g/L NaCl was 3.2±0.2, 3.3±0.1, 3.6±0.1, 4.6±0.2,

232   respectively, while the ORP was in the range of 480-510 mV vs Ag/AgCl. According to the iron

233   pourbaix diagram, the measured pH-ORP pairs in the 50, 100 and 200 g/L NaCl leaching solutions lay

234   on the edge between solid iron phases and soluble $FeCl^+$ (Figure S6).

235   Gypsum was dehydrated in the presence of NaCl in the lixiviants (Figure 2D) and upon increasing

236   leaching temperature, converted to highly oriented anhydrite ($CaSO_4$) crystals (Figure 2A). The release

237   of Ca can only be associated to the dissolution of $CaSO_4$ in water (*i.e.* about 10%), independently of the

238   chloride concentration, because the anion exchange reaction of $CaSO_4$ with chloride (eq. 4) at 200 °C

239   is not thermodynamically favorable.

240   (4) $CaSO_4 + Cl^- \rightleftharpoons CaCl^+ + SO_4^{2-}$ $\Delta G_{200°C}$= 52.8 kJ
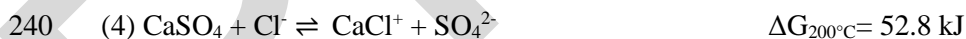
241   Ca leaching was influenced by temperature, as it firstly increasing up to 100 °C to then decrease again

242   to a minimum at 200 °C. This behavior is complex and needs to be correlated to three factors: pH of the

243   leachates, retrograde solubility of $CaSO_4$, and sulfate concentration. In fact, upon increasing the

244   leaching temperature the pH decreased, from about 6 at 50 °C to 4.6 at 200 °C, leading to a theoretical

245   increment of Ca leaching from gypsum/anhydrite structures. On the other hand, the solubility product

246   of $CaSO_4$ decreases with increasing temperature. Furthermore, the SO_4^{2-} concentration increases with

247   temperature due to the decomposition of jarosite (eq. 2, 3), which inhibits $CaSO_4$ dissolution according

248   to Le Chatelier's principle.

249   The leaching efficiencies of Cd, Cu, Pb, and Zn significantly increased with increasing NaCl

250   concentration and temperature (Figure 1A,B). Upon addition of chlorine anions, complexation reactions

251   take place through progressive substitution of solvation shell water molecules by ligands, as expressed

252   by eq. 5 for divalent metals.

253   (5) $[Me(H_2O)_n]^{2+} + xCl^- \rightleftharpoons [MeCl(H_2O)_{n-x}]^{2-x} + H_2O$

254   At higher NaCl concentrations more Cd, Cu, Pb, and Zn convert into soluble chloride forms (Figure S

255   7), as eq. 5 is shifted to the right. Thermodynamic calculations (Figure S8) and experimental results

256   agreed that chloride complexation mechanisms were most favorable at 200 °C. Leaching at 200 °C -the

257   highest investigated temperature- with a sodium chloride concentration of 300 g/L for 30 min gave

258   extraction yields of 84.2±0.8%, 58±2%, 44.9±0.6% and 39±2% for Pb, Zn, Cu and Cd, respectively.

259   The chloride complex formation of Cd, Cu and Zn as a function of NaCl concentration showed two

260   different slope regions. The steep increase in Cd, Cu and Zn leachability between 0 and 50 g/L NaCl

261   (Figure 1A), as well as the linear increase in leachability of Cd and Zn with leaching temperature (Figure

262   1B), can be associated to the solubilization of these metals from easily accessible forms (*e.g.* sulphates)

263   and jarosite [42]. This latter showed the most pronounced increase in dissolution between 0 and 50g/L

264   NaCl at 220 °C, which was complete at 100 g/L (Figure 2 D).

265   However, concurrent Zn, Cd and Cu leaching from more stable mineral phases (*i.e.* franklinite-like

266   spinels, $ZnSiO_4$) can occur at NaCl> 50g/L. Franklinite diffraction peaks intensity decreased with

267   temperature and NaCl concentration (Figure 2B, D), which can relate to leaching of Zn, and maybe Cd

268   and Cu. The most accredited reactive pathway for franklinite decomposition in chloride systems is

269   expressed in eq. 6 [45] (Figure S9).

270   (6) $ZnFe_2O_4 + 2Cl^- + 2H^+ \rightleftharpoons ZnCl_2 + Fe_2O_3 + H_2O$
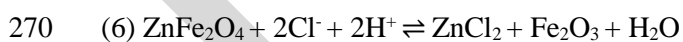
271   In fact, MW leaching solutions showed a gradual pH decreasing with applied leaching temperature,

272   which can promote franklinite decomposition, although the extent of the decomposition was limited.

273   The Zn leachability was highest after 30 min of reaction (58±2%) and decreased to 51.9±0.2% at 60

274   min. This behavior was reflected in the main XRD peak of franklinite (at about 41.2 2θ degrees) in the

275 residues (Figure 2 C), showing the lowest intensity after 30 min of leaching and a slightly higher

276 intensity after 60 min. This may suggest a partial re-crystallization of franklinite at longer MW leaching

277 time [46], although a dedicated study would be required to confirm such hypothesis, which is outside

278 the scope of this work. Cu and Cd extractions remained constant at 45-47% and 36-39%, respectively,

279 for all tested leaching times (Figure 1C).

280 The extraction of Pb followed yet another trend, whereby Pb conversion to soluble chlorides includes

281 an intermediate step in which barely soluble $PbCl_2$ formed. The formation of $PbCl_2$ influenced the

282 extraction trend of Pb from goethite and was supported by thermodynamic calculations. The latter

283 indicated that $PbSO_4$ scarcely dissolved in water as $Pb(SO_4)_2^{2-}$; whereas in NaCl solutions with a NaCl

284 concentration below 100 g/L the predominant insoluble species was $PbCl_2$; and at higher NaCl

285 concentrations (*i.e.* >100 g/L), $PbCl_3^{-}$ and $PbCl_4^{2-}$ species became progressively prevalent so that Pb

286 dissolution took place (Figure S10). Pb leachability was scarcely influenced by leaching time (Figure

287 1C). After 5 min, 83.2±0.1% of Pb was extracted, showing minor increments with time up to 90±1%

288 after 60 min.

289 In conclusion, the best Cd, Cu, Pb and Zn recoveries were achieved at elevated NaCl concentrations

290 (200-300 g/L) and temperatures (200 °C), with a negligible dissolution of iron and a limited (10%)

291 dissolution of calcium. In all the investigated conditions the As concentration in the leachates lied below

292 the ICP reporting limit (<350 ppb), indicating its presence in stable mineralogy.
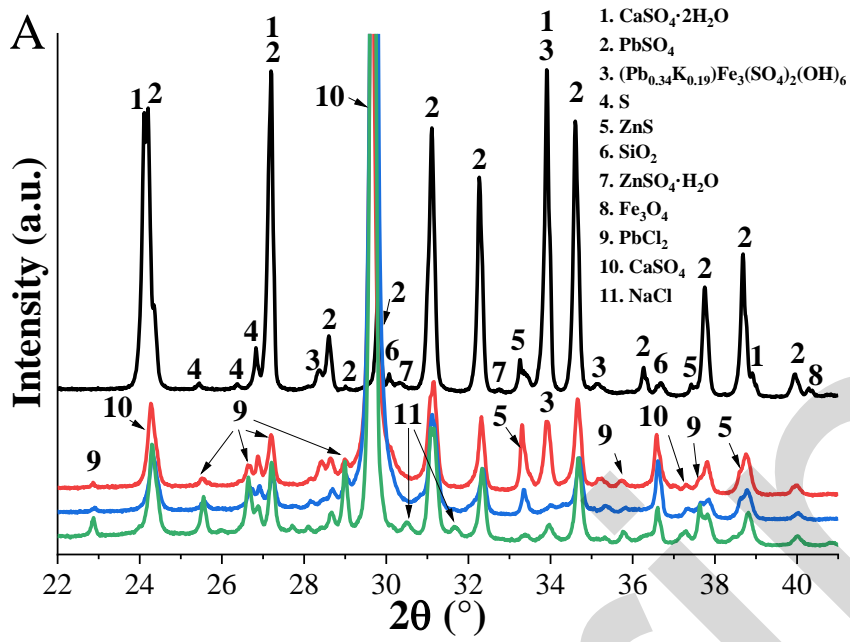
293 **3.3 Zn-leach product**

294 Zn-leach product was leached using three different lixiviants (NaCl 280 g/L, HCl 0.1 M + NaCl 280

295 g/L and HCl 1 M + NaCl 220 g/L) at three different temperatures (50, 100 and 200 °C) under microwave

296 irradiation. Upon addition of 1 M HCl, a lower NaCl concentration (220 g/L vs. 280 g/L) was used to

297 avoid oversaturation of the solution in NaCl. As for the goethite sludge (see above), first the leachability

298 of matrix elements, Ca, Fe and Si, will be discussed, followed by that of the valuable metals (Pb, Zn,

299 Ag, Bi, Sb) and contaminants (As, Cd, Cu). The achieved leachabilities and the mineralogy of the leach

300 residues are represented in Figures 3 and 5, and Figure 4, respectively.
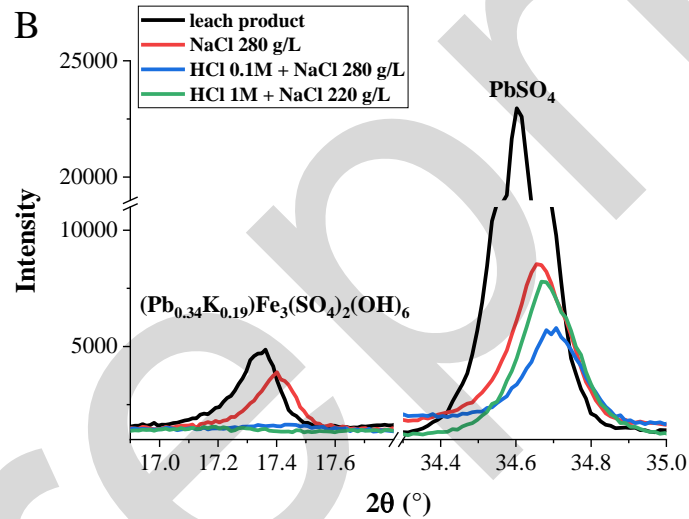
301
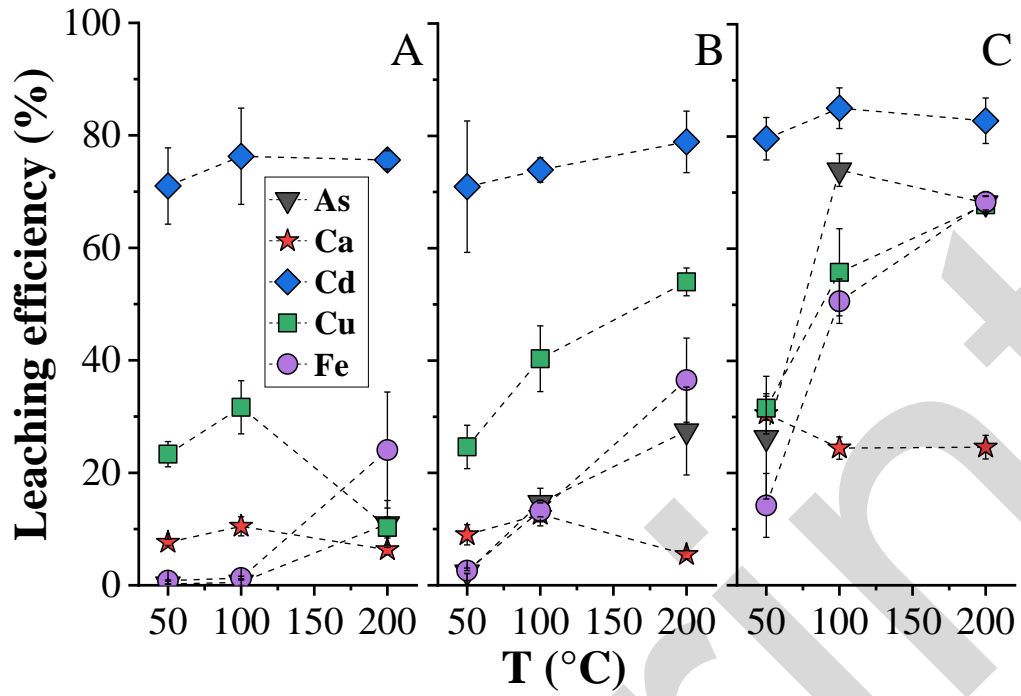
Figure 3: Leaching efficiency after MW leaching for As, Ca, Cd, Cu, and Fe from Zn-leach product using NaCl 280 g/L (A), HCl 0.1M + NaCl 280 g/L (B), and HCl 1M + NaCl 220 g/L (C) at three different temperatures (50, 100,200°C) for 5+30 min. Dotted lines are shown as a guide for the eye.

305

306

307
308

309   Figure 3: *XRD patterns of Zn-leach product, Zn-leach product after MW leaching with NaCl 280g/L,*
310   *with HCl 0.1M + NaCl 280g/L, and with HCl 1M + NaCl 220g/L (A). XRD details of anglesite, PbSO4*
311   *and plumbojarosite, $(Pb_{0.34}K_{0.19})Fe_3(SO_4)_2(OH)_6$ (B);cotunnite, $PbCl_2$, sulfur, S and sphalerite, ZnS (C).*
312

313

314   *Figure 4: Leaching efficiency after MW leaching for Ag, Bi, Pb, Sb, and Zn from Zn-leach product*
315   *using NaCl 280 g/L (A), HCl 0.1M + NaCl 280 g/L (B), and HCl 1M + NaCl 220 g/L (C) at three*
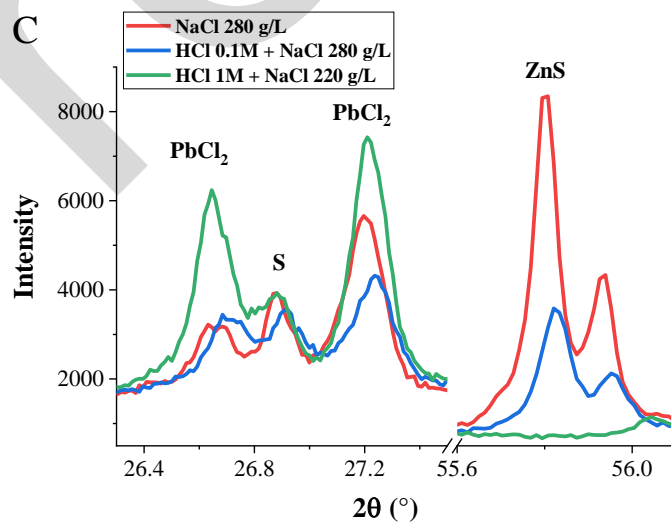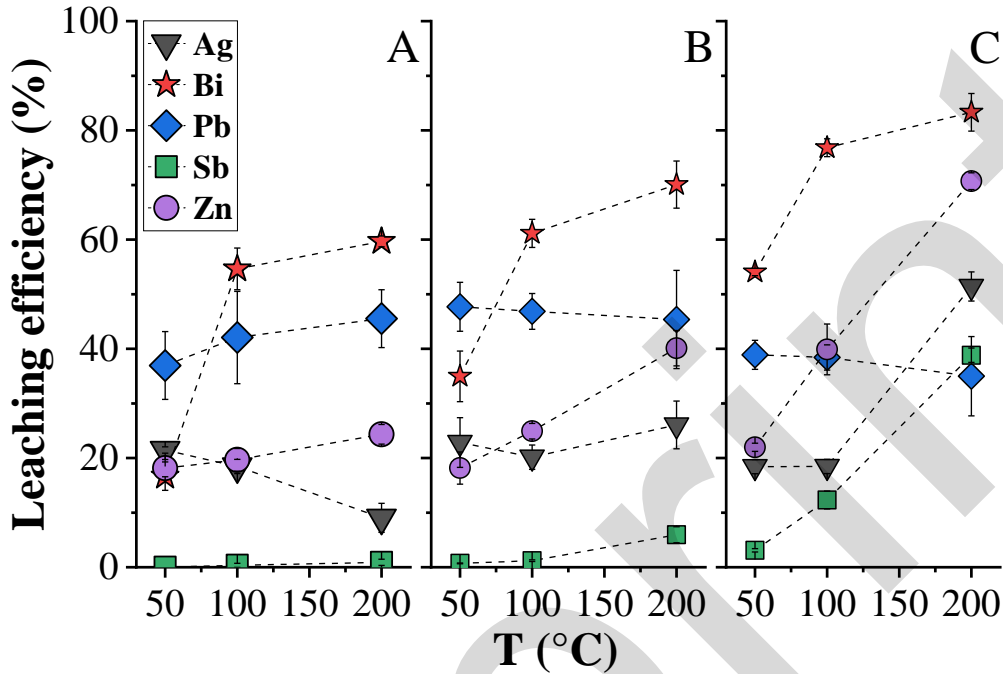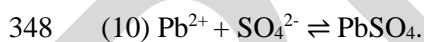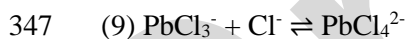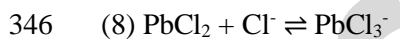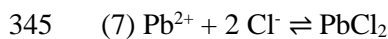316   *different temperatures (50, 100,200°C) for 5+30 min. Dotted lines are shown as a guide for the eye.*

317

318   The leachability of Ca and Fe increased upon addition of HCl to the NaCl leaching system. Calcium

319   sulfate solubility increased with acidity and decreased with increasing temperature (Figure 3). While,

320   Fe dissolution originated from Fe_3O_4 and jarosite phases increased upon increasing acidity and/or

321   temperature. Addition of 1 M HCl to the lixiviant strongly increased the Fe and Ca leachability, whereas

322   in the presence of 0.1 M HCl their leachabilities remained moderate, even at 200 °C. Furthermore, the

323   leachability of Si lied below 1.5% for all tested conditions.

324   The Zn-leach product is Pb-rich and the understanding of the $PbSO_4$ (anglesite) behavior is of primary

325   interest from economic and environmental point of view. According to thermodynamic simulations, at

326   elevated concentration of Cl^- (>5 M) and Pb^{2+} (≈14 g/L), the leaching pH controls the speciation of Pb

327   (Figure S11). At pH = 1 there is a transition zone wherein $PbSO_4$ or $PbCl_2$, $PbCl_3^-$ and $PbCl_4^{2-}$ result

328   more stable. Whereas, at pH > 1, $PbSO_4$ is predominant and at pH < 1 Pb-Cl species are favored. The

329 sulfate concentration instead increases the stability of $PbSO_4$ at lower pH and regulates the equilibrium

330 between $PbCl_2$, $PbCl^{3-}$ and $PbCl_4^{2-}$. At high SO_4^{2-} concentration the soluble Pb-Cl species become

331 prevalent (Figure S11). The formation of $PbCl_4^{2-}$ is promoted at high leaching temperatures and will

332 thus increase the solubilities of stable $PbSO_4$ and $PbCl_2$ [31]. Actually, during the leaching experiments

333 precipitation of $PbSO_4$ and $PbCl_2$ took place and was confirmed by XRD (Figure 4) and SEM/EDX

334 (Figure S12) analyses. Consequentially, the effects of HCl addition and temperature on Pb extraction

335 were mitigated by re-precipitation, leveling the Pb extraction to a maximum of 48±4% and 47±3%,

336 which were obtained with HCl 0.1 M + NaCl 280g/L at 50 and 100 °C, respectively (Figure 5). The

337 relative amounts of anglesite and cotunnite in the residue, as well as the concentration of Pb measured

338 by XRF, were the lowest after HCl 0.1 M + NaCl 280g/L leaching (Table 2). In fact, when Zn-leach

339 product was leached with NaCl 280 g/L the pH ($\approx$ 2.5) limited the dissolution of anglesite. While, for

340 HCl 1 M + NaCl 220g/L leaching, the pH ($\approx$ -0.5) promoted the formation of insoluble $PbCl_2$ (Table

341 2). Whereas, the pH during HCl 1 M + NaCl 220g/L leaching (pH$\approx$ 1) gave the best Pb extraction. At

342 this latter pH value, the lead species $PbCl_3^-$, $PbCl_4^{2-}$, $PbCl_2$ and $PbSO_4$ coexist, in agreement with the

343 thermodynamic calculations that yielded negative Gibbs free energy for all eq. 7-10 (Figure S13), with

344 anglesite as the most favored product, followed by $PbCl_4^{2-}$.

345 (7) $Pb^{2+} + 2\ Cl^- \rightleftharpoons PbCl_2$

346 (8) $PbCl_2 + Cl^- \rightleftharpoons PbCl_3^-$

347 (9) $PbCl_3^- + Cl^- \rightleftharpoons PbCl_4^{2-}$

348 (10) $Pb^{2+} + SO_4^{2-} \rightleftharpoons PbSO_4$.

349 *Table 2: XRD Rietveld refining of Pb-containing phases (%), residual Pb (%) in the leaching residues*
350 *and leached mass from the Zn-leach product (%) after MW leaching at 200 °C, for 5+30 min.*

Lixiviant	Anglesite $PbSO_4$	Cotunnite $PbCl_2$	Plumbojarosite $(Pb_{0.34}K_{0.19})Fe_3(SO_4)_2(OH)_6$	Pb (%) *XRF of residues*	Leached mass (%)
NaCl 280 g/L	16.3%	1.9%	17.5%	12.15 ±0.02	37.1 ±0.5
HCl 0.1M + NaCl 280 g/L	13.4%	1.3%	1.8%	5.359 ±0.002	45.5 ±0.8
HCl 1M + NaCl 220 g/L	21.5%	6.8%	2.5%	7.80 ±0.06	53 ±2

351 Furthermore, at lower pH plumbojarosite undergoes decomposition, which provides an additional

352 amount of soluble Pb in the HCl-containing leachates [49]. However, when dissolved $[SO_4^{2-}]$ increased,

353 the stability zone of $PbSO_4$ extended. Such increase occurred due to the decomposition of

354 plumbojarosite and ZnS and dissolution of $CaSO_4$ (Figure 3) upon increasing leaching temperature and

355 decreasing pH. Therefore, the thermodynamic advantage of temperature toward the formation of $PbCl_4^{2-}$

356 was counterbalanced by reprecipitation phenomena. $PbSO_4$ and $PbCl_2$ solubilities increase with

357 temperature but when the MW reactors are cooled again to room temperature these compounds tend to

358 reprecipitate as white crystals at the top of the settled solids. Also, at 200 °C, the conversion of $PbSO_4$

359 to $PbCl_2$ could be controlled by diffusion of Cl^- through emerging $PbCl_2$ or oxidized $PbO_{1-x}Cl_{2x}$ surface

360 layers [50]. Finally, leaching tests at room temperature showed good Pb solubilization with less

361 pronounced reprecipitation for all tested conditions, with a maximum leachability of 84% in HCl 0.1 M

362 + NaCl 280 g/L (Table S1).

363 In addition to Pb, the potential value of Zn-leach product resides in Ag, Bi, Sb and Zn. Their observed

364 leaching efficiencies during MW leaching tests for 30 min are represented in Figure 5. The Bi extraction

365 in 280 g/L NaCl increased significantly up to 60±1% upon increasing the leaching temperature to 200

366 °C (Figure 5A). Furthermore, HCl addition enhanced the Bi extraction up to 83±3% at 200 °C in HCl

367 1M + NaCl 220 g/L (Figures 5B, C). The extraction of Bi as function of temperature evidenced two

368 distinct slope regions. The sharp increment below 100 °C might be associated to the solubilization of

369 Bi-bearing soluble mineral phases, while above 100 °C the increment became more gradual and might

370 be associated to less soluble mineral phases, likely Pb-jarosite and $PbSO_4$ which showed enhanced

371 decomposition with temperature and acidity (Figure 4B).

372 Increasing leaching temperature and acidity was also advantageous for Sb extraction, which reached a

373 maximum of 39±1% at 200 °C at low pH in 1 M HCl + 220 g/L NaCl. Zn leaching showed the same

374 dependence on temperature and acidity and about 20% of Zn resulted readily soluble in all the tested

375 leaching systems, which can be related to the presence of water soluble gunningite, $ZnSO_4 \cdot H_2O$. The

376 best Zn leachability was obtained at 200 °C and increased with the applied HCl concentration (69±2%

377 with 1 M), whereas the XRD signal of ZnS in the residue decreased (Figure 4C). Given that both Sb

378 and Zn leaching efficiencies increased linearly with leaching temperature (Figure S14) and their

379 leachabilities are statistically correlated with an R^2 value of 0.9055 (Table 3, Figure S15), suggests an

380 association of both elements in the same mineral phase, which is likely sphalerite [47]. The

381 solubilization of metal sulfides at hydrothermal conditions (P > 1 atm, T > 120 °C) is associated to the

382 oxidation of S, as represented by eq. 11-12 [7,48]. Both temperature and acidity are beneficial for the

383 decomposition of sphalerite. On the one side, a higher processing temperature generates a higher

384 autogenous pressure inside the vessel, and thus a higher O_2 partial pressure. On the other side, acid is

385 needed to promote the oxidation of sulfidic phase and the liberation of metallic species, eq. 11.

386 (11) $ZnS + 0.5O_2 + 2H^+ \rightleftharpoons Zn^{2+} + S^0 + H_2$

387 (12) $S^0 + 0.5O_2 + H_2O \rightleftharpoons 2H^+ + SO_4^{2-}$
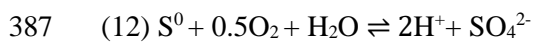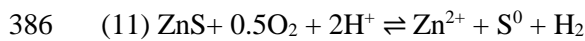
388 *Table 3: Spearman correlation and p-value derived from the statistical analysis.*

		Ag	As	Bi	Ca	Cd	Cu	Fe	Pb	Sb	Zn
Ag	*Spearman Corr.*	1	0.14271	0.20764	0.01446	-0.06405	0.47831	0.19731	-0.4845	0.20561	0.24793
	p-value	--	0.57214	0.40836	0.95458	0.80066	0.04466	0.43257	0.04158	0.41307	0.32121
As	*Spearman Corr.*	0.14271	1	0.81388	0.44369	0.45952	0.73755	0.91106	-0.14648	0.92908	0.84889
	p-value	0.57214	--	1.58E-09	0.00672	0.00481	2.87E-07	1.22E-14	0.39395	3.00E-16	6.10E-11
Bi	*Spearman Corr.*	0.20764	0.81388	1	0.19382	0.4592	0.77941	0.90245	-0.08134	0.83545	0.94981
	p-value	0.40836	1.58E-09	--	0.25735	0.00484	2.14E-08	5.50E-14	0.63722	2.33E-10	9.88E-19
Ca	*Spearman Corr.*	0.01446	0.44369	0.19382	1	0.51145	0.42033	0.24556	-0.17272	0.43064	0.21647
	p-value	0.95458	0.00672	0.25735	--	0.00143	0.0107	0.14886	0.31378	0.00875	0.20476
Cd	*Spearman Corr.*	-0.06405	0.45952	0.4592	0.51145	1	0.47079	0.3897	0.17889	0.5208	0.50862
	p-value	0.80066	0.00481	0.00484	0.00143	--	0.00376	0.0188	0.29652	0.00113	0.00154
Cu	*Spearman Corr.*	0.47831	0.73755	0.77941	0.42033	0.47079	1	0.69781	-0.22831	0.79102	0.76963
	p-value	0.04466	2.87E-07	2.14E-08	0.0107	0.00376	--	2.24E-06	0.18047	9.39E-09	4.11E-08
Fe	*Spearman Corr.*	0.19731	0.91106	0.90245	0.24556	0.3897	0.69781	1	-0.12921	0.87265	0.91403
	p-value	0.43257	1.22E-14	5.50E-14	0.14886	0.0188	2.24E-06	--	0.4526	4.03E-12	7.03E-15
Pb	*Spearman Corr.*	-0.4845	-0.14648	-0.08134	-0.17272	0.17889	-0.22831	-0.12921	1	-0.15836	-0.01441
	p-value	0.04158	0.39395	0.63722	0.31378	0.29652	0.18047	0.4526	--	0.35629	0.9335
Sb	*Spearman Corr.*	0.20561	0.92908	0.83545	0.43064	0.5208	0.79102	0.87265	-0.15836	1	0.84423
	p-value	0.41307	3.00E-16	2.33E-10	0.00875	0.00113	9.39E-09	4.03E-12	0.35629	--	9.84E-11
Zn	*Spearman Corr.*	0.24793	0.84889	0.94981	0.21647	0.50862	0.76963	0.91403	-0.01441	0.84423	1
	p-value	0.32121	6.10E-11	9.88E-19	0.20476	0.00154	4.11E-08	7.03E-15	0.9335	9.84E-11	--

2 tailed test of significance used

389

390 The Ag leachability showed an unusual trend, as in the absence of HCl the leachability decreased with

391 increasing temperature, whereas in the presence of 0.1 M HCl it remained constant at each temperature

392 at about 20% and in 1 M HCl it increased to 52±3% at 200 °C. The modeling of a Ag-Cl system at [Cl⁻

393   ]= 5 M showed that acidity and temperature had a minor effect on the solubilization of Ag as $AgCl_2^-$,

394   $AgCl_3^{2-}$, $AgCl_4^{3-}$ (Figure S16). Thus, the silver solubility was determined by its initial mineralogical

395   occurrence and/or co-precipitation during reaction. In this sense, it should be mention that the formation

396   of small amounts of precipitate in the leachates after filtration over time in all tested conditions was

397   observed. A mixture of dried solid precipitates, collected from different experiments, was chemically

398   (XRF) and mineralogically (XRD) characterized and showed the presence of $PbSO_4$ (Pb=51-52% wt.)

399   and $CaSO_4 \cdot 2H_2O$ as main components and the inclusion of other elements, such as Ag (0.3%), As (4%),

400   Cl (1%) and Si (1%). Therefore, fractions of extracted silver may co-precipitate.

401   The removal of Cd was remarkable, giving leaching efficiencies between 70 and 85% (Figure 3) at any

402   temperature and acidity, indicating its presence in Zn-leach product as absorbed cation or water-soluble

403   species. As and Cu followed analogous leaching trends with temperature at 0.1 M and 1 M HCl

404   concentrations, suggesting a mineral association. Actually, a scatterplot matrix of leaching efficiencies

405   (Figure S15) showed indeed potential linear correlations, including, for example, Fe-Zn (R^2=0.8622)

406   and As-Fe (R^2=0.8111) pairs. The outcomes of the statistical analysis (Table 3) evidenced a correlation

407   ($p<0.001$) for the As, Bi, Cu, Fe, Sb, and Zn leachabilities, which may indicate the co-occurrence of

408   such metals in the same mineral phases. At the light of the correlations and the leaching trends, Sb and

409   Zn seemingly coexisted in sphalerite, ZnS, as discussed above. While, As, Bi, Cu, and Fe can be

410   associated either in Fe-containing species (Fe_3O_4 and jarosite) or sulphides, which showed comparable

411   dissolution vs temperature and acidity. While the leachability of Ag, Ca, Cd, and Pb showed weaker

412   correlations with that of other elements.

413   In conclusion, for all tested lixiviants on the Zn-leach residue the optimal microwave leaching

414   temperature was 200 °C as the leachability of the target metals (Ag, Bi, Sb, Zn, Cd) was highest.

415   However, the selection of the most suitable lixiviant needs to be contextualized to the purpose of the

416   leaching, which might be the metal recovery and/or the decontamination of the Zn-leach product.

417   Depending on the chosen aim, the metal leaching selectivity might be relevant. Therefore, leaching in

418   280 g/L NaCl gave the most selective leaching for Ag, Bi, Pb and Zn, but leaching efficiencies were

419   moderate; whereas upon addition of 1 M HCl to 220 g/L NaCl, the extraction of all target metals (Ag,

420   Pb, Zn, Sb and Bi) was highest but selectivity dropped as matrix elements (Ca, Fe), as well as

421   contaminants (As, Cd, Cu), also dissolved. The system HCl 0.1 M + NaCl 280 g/L gave the best balance

422   of acidity and chloride concentration for the recovery of Pb at temperatures below 100 °C, although Pb

423   removal/recovery was generally not satisfactory (≈50%). The best Ag extraction was just above 50% at

424   200 °C with HCl 1 M + NaCl 220 g/L.

425   **3.4 Microwave assisted leaching: advantages and limitations**

426   In this work a laboratory microwave digester equipped with pressure sealed reactors was used. Such

427   system allows to perform autoclave leaching at hydrothermal conditions (*i.e.* leaching at temperatures

428   above the boiling point of water, 100 °C, and at elevated autogenous pressure [52]).

429   If compared with conventional heating, the MW heating rate is faster and more efficient, with potential

430   increase of productivity, by decreasing processing times [37]. Actually, the studied reaction systems

431   were able to reach 200 °C in 5 min through MW absorption, whereas, after 10 min (*i.e.* 5 min heating

432   + 5 min dwelling) of treatment at 200 °C, the 300 g/L NaCl system already reached a plateau zone for

433   all metal extraction values from goethite sludge.

434   During MW heating the water molecules (dipoles) couple with MWs, which in response heat up through

435   dielectric loss mechanisms, generating direct heating at molecular level of aqueous systems [34]. To

436   evaluate the NaCl microwave assisted leaching in terms of energy balance it is noteworthy to mention

437   that the higher the NaCl concentration in solution the more MW power must be supplied to obtain the

438   same temperature profile (SI, Figure S17). In fact, the dissolved Na^+ and Cl^- ions coordinate water

439   molecules, which are thus not acting anymore as free dipoles [54], and hinder the dielectric loss

440   mechanisms.

441   In the studied systems it was unlikely that the treated solid materials heated also through MW

442   absorption, as the measured dielectric constant (ε') and loss factor (ε'') at 25 °C, 1.8-2.6 GHz of both

443   goethite sludge and Zn-leach product were low compared to those of MilliQ water , NaCl 280 g/L , and

444   HCl 1M + 220 g/L (Table 4). Thus, the heating effect of MW coupling with solids might be considered

445   negligible compared to the heating effect of the aqueous systems. Therefore, it was deemed unlikely

446   that micro-crack formation [35,36,55,56] or mineral liberation due to MW heating of the mineral

447   materials occurred, as experimental proof of such behavior was not observed *i.e.* by SEM/EDX analysis

448   of residues.

449   *Table 4: Measured dielectric properties of the main materials used in this work at 25 °C, at the MW*
450   *frequency 1.8-2.6 GHz.*

Material	Dielectric constant, ε'	Dielectric loss, ε"
Goethite sludge (dried)	1.83	3.49
Zn-leach product (dried)	0.05	0.15
MilliQ water	76.28	8.18
NaCl 280 g/L solution	137.55	0.77
HCl 1 M + 220 g/L solution	137.62	1.89

451

452   The effect of microwaves on the chemistry of leaching processes is generally difficult to study, because

453   of different heating rates, potential inhomogeneity of temperatures and temperature measurement

454   limitations. Proper investigation of leaching results obtained on sphalerite showed comparable

455   activation energies in both conventional and MW leaching and minor effect on the reaction chemistry

456   [57].

457   Conventionally heated autoclave leaching is widely applied on industrial scale for processing of sulfidic

458   ores [53], but nowadays the use of MW at industrial scale for such application is still limited. In fact,

459   the cheaper and more mature microwave technology makes use of magnetrons working at 2.45 GHz.

460   At this frequency the penetration depth (the maximum distance the microwaves can run through the

461   aqueous solutions) is commonly limited to a few centimeters, which is a substantial limitation to the

462   processing of large amounts of material. However, huge effort undertaken by engineers to enhance the

463   reactor geometry, mixing, and fluid dynamics has allowed to produce off-the-shelf liter-scale MW

464   reactors (*e.g.* Anton Paar, Milestone). Alternatively, the 915 MHz frequency can be used, which can

465   provide penetration depths of tens of centimeters. Magnetrons working at this frequency are more

466   expensive, though. Furthermore, stop-flow MW reactors can be a possible solution [58], which have

467   been successfully applied in organic chemistry to increase productivity.

3.5 Environmental evaluation of leach residues

The water leachability of the starting materials goethite sludge, Zn-leach product and the chosen Cl-leach residues from both materials was tested. The obtained leachabilities at L/S = 10 could be compared to the limiting values for use as non-shaped construction material as reported in the Flemish VLAREMA legislation [59] as well as newly proposed legislative values which currently are not yet applied [60]. Table 5 shows the obtained cumulative emissions at L/S = 10 as measured by the one stage batch leaching test. The leachabilities of Cd, Cu, Ni and Zn were exceeding the limit values proposed by the current Flemish legislation, for both starting materials. Furthermore, Pb and Cr were above the threshold limit for the Zn-leach product, as well as Sb and Co exceeded the new proposed values. It must be noted that the Cd, Cu and Zn leachability for both the goethite residue and Zn-leach product drastically decreased after treatment by MW leaching, but their leachability was still exceeding the legislative limit values. On the contrary, Ni released from the MW leached materials respected the normative. Cr and Co leachability from the treated Zn-leach product also decreased to below their limit value. However, Pb leaching was even higher than from the starting material itself, potentially due to the solubilization of $PbCl_2$.

483 *Table 5: Cumulative emissions of goethite sludge, Residue 1 from MW leaching of the goethite (NaCl*
484 *300 g/L, 200 °C, 5+30 min), Zn-leach product, and Residue 2 from MW leaching of the Zn-leach*
485 *product HCl 0.1M + NaCl 280 g/L, 200 °C, 5+30 min) at L/S = 10 measured by the one stage batch*
486 *leaching test. The emissions are compared to the VLAREMA limiting values for use as non-shaped*
487 *construction material.*

Cumulative emission at L/S = 10 (mg/kg)

Element	Goethite sludge	Residue 1	Leach-product	Residue 2	VLAREMA Appendix 2.3.2.B	Proposed new legislative values
As	<0.35	<0.35	<0.35	<0.35	0.8	0.8
Cd	27	0.18	1900	2.5	0.03	0.03
Cr	<0.12	<0.12	2.4	<0.12	0.5	2.6
Cu	0.67	0.57	560	1.8	0.5	0.8
Pb	<0.25	<0.25	22	29	1.3	1.3
Ni	0.76	<0.2	5.3	<0.2	0.75	0.75
Zn	26000	35	75000	21	2.8	2.8
Sb	<1	<1	2.4	1.3		1
Ba	0.26	<0.01	0.13	<0.01		20
Co	0.20	0.08	0.85	0.15		0.5
Mo	<0.1	<0.1	<0.1	<0.1		55
Se	<0.75	<0.75	<0.75	<0.75		2
Sn	<0.5	<0.5	<0.5	<0.5		1
V	<0.08	<0.08	<0.08	<0.08		2.5
pH	6.07	6.74	3.20	4.66		

488

489 For the other investigated heavy metals (Ba, Mo, Se, Sn, V) the leaching behavior was below the values

490 proposed for the future Flemish normative.

491 In conclusion, although the heavy metal leachability of the MW leached materials lies drastically lower

492 than their starting materials they cannot be applied as non-shaped construction materials according to

493   Flemish legislation. However, due to the strong decrease in leachability further research in stabilization

494   (*e.g.* by use as aggregate in concrete) of the metals in the material might be opportune.

4. Conclusions

496

497   Chloride leaching of two zinc plant residues, goethite sludge and zinc leach product, was shown to give

498   selective leaching of valuable and heavy metals with the aim to recover metals and decontaminate the

499   matrix, respectively. Furthermore, microwave assisted leaching confirmed to be a fast and effective tool

500   to enhance hydrometallurgical extraction. The fast heating was mainly associated to the interaction of

501   MWs with the aqueous solutions. Whereas, MW interaction with the solid zinc plant residues was

502   limited due to their poor dielectric properties.

503   For goethite sludge Cd, Cu, Pb, and Zn were extracted selectively from Fe (<0.06%) in a NaCl solution.

504   A higher NaCl concentration (300 g/L) and/or temperature (200 °C) increased the leachability of Cd,

505   Cu, Pb, and Zn for 30 min leaching. The best Pb leaching was achieved with NaCl 280 g/L at 200 °C

506   for 1 h. This is a selective route, which makes use of cheap reagents, as first decontamination stage for

507   this material. Even though the cumulative emission of Cd, Cu and Zn from the MW leached goethite

508   sludge was considerably decreased, their leachability still exceeded the leaching limit values of the

509   Flemish legislation for use of the material as non-shaped construction material.

510   MW leaching of Bi, Sb, and Zn from the Zn-leach product was most effective at high leaching

511   temperature (200 °C). Bi can be extracted from this residue in a NaCl solutions to an attractive extent

512   (60%), but was optimized to 83% through addition of 1 M HCl to the NaCl solution. This latter lixiviant

513   composition also achieved the best Ag extraction (52±3%) at 200 °C.

514   Contrarily, Pb leaching from the Zn-leach product was more pronounced at low leaching temperature

515   (room temperature experiments gave best Pb leachability) because anglesite and cotunnite

516   reprecipitation at higher temperatures was likely triggered by temperature variation (during and after

517   MW leaching).

518   In HCl 0.1 M + NaCl 280 g/L the concentration of hydrogen, chloride and sulfate ions are well balanced

519   to achieve the best Pb extractions in the all the examined leaching conditions. The limited solubilization

520   of Pb is a factor that may limit the application of such treatment for the valorization of the residue.

521   However, a second leaching stage can be introduced to enhance Pb recovery.

522   The environmental impact highlighted an enhanced mobility of the Pb after the MW treatment of the

523   Zn-leach residue, limiting the application as non-shaped construction material, even though a significant

524   reduction in leachability for other polluting metals was noticed.

525 Acknowledgments

530 Conflict of interest

531   There is no conflict of interest to declare.

532 References

533

534 [1]   K. Venkateswarlu, R. Nirola, S. Kuppusamy, P. Thavamani, R. Naidu, M. Megharaj, Abandoned
535   metalliferous mines: ecological impacts and potential approaches for reclamation, Rev. Environ.
536   Sci. Biotechnol. 15 (2016) 327–354. doi:10.1007/s11157-016-9398-6.
537 [2]   V. Hatje, R.M.A. Pedreira, C.E. De Rezende, C.A.F. Schettini, G.C. De Souza, D.C. Marin, P.C.
538   Hackspacher, The environmental impacts of one of the largest tailing dam failures worldwide,
539   Sci. Rep. 7 (2017) 1–13. doi:10.1038/s41598-017-11143-x.
540 [3]   Tayebi-Khorami, Edraki, Corder, Golev, Re-Thinking Mining Waste Through an Integrative
541   Approach Led by Circular Economy Aspirations, Minerals. 9 (2019) 286.
542   doi:10.3390/min9050286.
543 [4]   S. Deetman, S. Pauliuk, D.P. Van Vuuren, E. Van Der Voet, A. Tukker, Scenarios for Demand
544   Growth of Metals in Electricity Generation Technologies, Cars, and Electronic Appliances,
545   Environ. Sci. Technol. 52 (2018) 4950–4959. doi:10.1021/acs.est.7b05549.
546 [5]   European Commission, Extractive Waste, Environment. (2018). doi:10.1002/hyp.1051.
547 [6]   F. Habashi, Recent trends in extractive metallurgy, J. Min. Metall. Sect. B Metall. 45 (2009) 1–
548   13. doi:10.2298/JMMB0901001H.
549 [7]   F. Habashi, Textbook of Hydrometallurgy, Second Edi, 1999.
550 [8]   M. Şahin, M. Erdem, Cleaning of high lead-bearing zinc leaching residue by recovery of lead
551   with alkaline leaching, Hydrometallurgy. 153 (2015) 170–178.
552   doi:10.1016/j.hydromet.2015.03.003.
553 [9]   P.T. Davey, T.R. Scott, Removal of iron from leach liquors by the "Goethite" process,
554   Hydrometallurgy. 2 (1976) 25–33. doi:10.1016/0304-386X(76)90011-6.
555 [10]   Z. Youcai, R. Stanforth, Integrated hydrometallurgical process for production of zinc from
556   electric arc furnace dust in alkaline medium, J. Hazard. Mater. 80 (2000) 223–240.
557   doi:10.1016/S0304-3894(00)00305-8.

558 [11] S.M.J. Koleini, H. Mehrpouya, K. Saberyan, M. Abdolahi, Extraction of indium from zinc plant
559 residues, Miner. Eng. 23 (2010) 51–53. doi:10.1016/j.mineng.2009.09.007.
560 [12] W. Wang, F. Wang, F. Lu, Microwave alkaline roasting-water dissolving process for germanium
561 extraction from zinc oxide dust and its analysis by response surface methodology (RSM), Metall.
562 Res. Technol. 115 (2018) 203. doi:10.1051/metal/2017093.
563 [13] K. Binnemans, P.T. Jones, B. Blanpain, T. Van Gerven, Y. Pontikes, Towards zero-waste
564 valorisation of rare-earth-containing industrial process residues: A critical review, J. Clean.
565 Prod. 99 (2015) 17–38. doi:10.1016/j.jclepro.2015.02.089.
566 [14] A. Di Maria, K. Van Acker, Turning Industrial Residues into Resources: An Environmental
567 Impact Assessment of Goethite Valorization, Engineering. 4 (2018) 421–429.
568 doi:10.1016/j.eng.2018.05.008.
569 [15] L. Tang, C. Tang, J. Xiao, P. Zeng, M. Tang, A cleaner process for valuable metals recovery
570 from hydrometallurgical zinc residue, J. Clean. Prod. 201 (2018) 764–773.
571 doi:10.1016/j.jclepro.2018.08.096.
572 [16] C.A. Pickles, O. Marzoughi, Thermodynamic investigation of the sulphation roasting of electric
573 arc furnace dust, Minerals. 9 (2019). doi:10.3390/min9010018.
574 [17] G. min Jiang, B. Peng, Y. jie Liang, L. yuan Chai, Q. wei Wang, Q. zhu Li, M. Hu, Recovery of
575 valuable metals from zinc leaching residue by sulfate roasting and water leaching, Trans.
576 Nonferrous Met. Soc. China (English Ed. 27 (2017) 1180–1187. doi:10.1016/S1003-
577 6326(17)60138-9.
578 [18] M. Swain, K.K. Sahu, B.N. Roy, Recycling of Jarosite For Recovery of Valuable Metals and its
579 Utilisation, Int. J. Sci. Tech. Res. Eng. Www.Ijstre.Com. 1 (2016) 36–46. www.ijstre.com.
580 [19] R. Raghavan, P.K. Mohanan, S.C. Patnaik, Innovative processing technique to produce zinc
581 concentrate from zinc leach residue with simultaneous recovery of lead and silver,
582 Hydrometallurgy. 48 (1998) 225–237. doi:10.1016/S0304-386X(97)00082-0.
583 [20] N. Kazakova, B. Lucheva, P. Iliev, Modeling of H2SO4-NaCl leaching process of zinc ferrite
584 cake, J. Chem. Technol. Metall. 55 (2020) 417–428.
585 [21] Z.H. Guo, F.K. Pan, X.Y. Xiao, L. Zhang, K.Q. Jiang, Optimization of brine leaching of metals
586 from hydrometallurgical residue, Trans. Nonferrous Met. Soc. China (English Ed. 20 (2010)
587 2000–2005. doi:10.1016/S1003-6326(09)60408-8.
588 [22] B. Bahram, M. Javad, Chloride leaching of lead and silver from refractory zinc plant residue,
589 Res. J. Chem. Environ. 15 (2011) 473–480.
590 [23] M.D. Turan, H.S. Altundoğan, F. Tümen, Recovery of zinc and lead from zinc plant residue,
591 Hydrometallurgy. 75 (2004) 169–176. doi:10.1016/j.hydromet.2004.07.008.
592 [24] M. Li, S. Zheng, B. Liu, H. Du, D.B. Dreisinger, L. Tafaghodi, Y. Zhang, The leaching kinetics
593 of cadmium from hazardous Cu-Cd zinc plant residues, Waste Manag. 65 (2017) 128–138.
594 doi:10.1016/j.wasman.2017.03.039.
595 [25] T. Havlik, B. Friedrich, S. Stopic, Pressure leaching of EAF dust with sulphuric acid, Erzmetall.
596 (2004) 113–120. http://www.metallurgie.rwth-
597 aachen.de/new/images/pages/publikationen/havlik_erzmetall_57_id_9401.pdf.
598 [26] Y. Hua, Z. Lin, Z. Yan, Application of microwave irradiation to quick leach of zinc silicate ore,
599 Miner. Eng. 15 (2002) 451–456. doi:10.1016/S0892-6875(02)00050-X.
600 [27] E. Güler, A. Seyrankaya, I. Cöcen, Hydrometallurgical evaluation of zinc leach plant residue,
601 Asian J. Chem. 23 (2011) 2879–2888.
602 [28] J. Vereš, Š. Jakabský, M. Lovás, S. Hredzák, Non-isothermal microwave leaching kinetics of
603 zinc removal from basic oxygen furnace dust, Acta Montan. Slovaca. 15 (2010) 204–211.
604 [29] M. Sethurajan, D. Huguenot, R. Jain, P.N.L. Lens, H.A. Horn, L.H.A. Figueiredo, E.D. van
605 Hullebusch, Leaching and selective zinc recovery from acidic leachates of zinc metallurgical
606 leach residues, J. Hazard. Mater. 324 (2017) 71–82. doi:10.1016/j.jhazmat.2016.01.028.
607 [30] M.M. Khosravirad, F. Bakhtiari, S. Ghader, E. Abkhoshk, An improved process methodology
608 for extracting cobalt from zinc plant residues, Hydrometallurgy. 191 (2020) 105163.
609 doi:10.1016/j.hydromet.2019.105163.
610 [31] H. Xie, L. Zhang, H. Li, S. Koppala, S. Yin, S. Li, K. Yang, F. Zhu, Efficient recycling of Pb
611 from zinc leaching residues by using the hydrometallurgical method, Mater. Res. Express. 6
612 (2019). doi:10.1088/2053-1591/ab11b9.

[32] R. Winand, Chloride hydrometallurgy, Hydrometallurgy. 27 (1991) 285–316. doi:10.1016/0304-386X(91)90055-Q.

[33] R.L. Zhang, X.F. Zhang, S.Z. Tang, A.D. Huang, Ultrasound-assisted HCl-NaCl leaching of lead-rich and antimony-rich oxidizing slag, Ultrason. Sonochem. 27 (2015) 187–191. doi:10.1016/j.ultsonch.2015.05.020.

[34] M. Al-Harahsheh, S.W. Kingman, Microwave-assisted leaching - A review, Hydrometallurgy. 73 (2004) 189–203. doi:10.1016/j.hydromet.2003.10.006.

[35] C.A. Pickles, Microwaves in extractive metallurgy: Part 1 - Review of fundamentals, Miner. Eng. 22 (2009) 1102–1111. doi:10.1016/j.mineng.2009.02.015.

[36] C.A. Pickles, Microwaves in extractive metallurgy: Part 2 - A review of applications, Miner. Eng. 22 (2009) 1112–1118. doi:10.1016/j.mineng.2009.02.014.

[37] L. Tian, Z. Xu, L. Chen, Y. Liu, T. an Zhang, Effect of microwave heating on the pressure leaching of vanadium from converter slag, Hydrometallurgy. 184 (2019) 45–54. doi:10.1016/j.hydromet.2018.11.004.

[38] OVAM, VITO, Emis, Compendium for sampling and analysis (CMA), (2014). https://emis.vito.be/nl/referentielabo-ovam.

[39] British Standards Institution, Characterisation of waste. Leaching. Compliance test for leaching of granular waste materials and sludges. One stage batch test at a liquid to solid ratio of 10 l/kg for materials with particle size below 10 mm (without or with size reduction), 2002.

[40] M. Quaghebeur, C. Kenis, P. Nielsen, K. Tirez, D. Geysen, D. Dedecker, Assessing the environmental quality of soils that are used in construction works: comparison of column and batch tests in a regulatory context, in: Wascon 2006 Sixth Int. Conf. Environ. Tech. Implic. Constr. with Altern. Mater. Sci. Eng. Recycl. Environ. Prot., 2006.

[41] U. Kalbe, W. Berger, J. Eckardt, F.G. Simon, Evaluation of leaching and extraction procedures for soil and waste, Waste Manag. 28 (2008) 1027–1038. doi:10.1016/j.wasman.2007.03.008.

[42] X.B. Min, X. De Xie, L.Y. Chai, Y.J. Liang, M. Li, Y. Ke, Environmental availability and ecological risk assessment of heavy metals in zinc leaching residue, Trans. Nonferrous Met. Soc. China (English Ed. 23 (2013) 208–218. doi:10.1016/S1003-6326(13)62448-6.

[43] S.J. Hock, Precipitation of Hematite and Recovery of Hydrochloric Acid from Aqueous Iron(II, III) Chloride Solutions by Hydrothermal Processing, (2009) 1–120.

[44] L. Chen, Thermal decomposition characterization of supergene potassium-jarosite and sodium-jarosite minerals from the northern Tibetan Plateau, China, Physicochem. Probl. Miner. Process. 54 (2018) 459–466. doi:https://doi.org/10.5277/ppmp1829.

[45] Š. Langová, J. Leško, D. Matýsek, Selective leaching of zinc from zinc ferrite with hydrochloric acid, Hydrometallurgy. 95 (2009) 179–182. doi:10.1016/j.hydromet.2008.05.040.

[46] C.G. Anchieta, E.C. Severo, C. Rigo, M.A. Mazutti, R.C. Kuhn, E.I. Muller, E.M.M. Flores, R.F.P.M. Moreira, E.L. Foletto, Rapid and facile preparation of zinc ferrite ($ZnFe_2O_4$) oxide by microwave-solvothermal technique and its catalytic activity in heterogeneous photo-Fenton reaction, Mater. Chem. Phys. 160 (2015) 141–147. doi:10.1016/j.matchemphys.2015.04.016.

[47] F.E. Minz, N. Bolin, P. Lamberg, K. Bachmann, J. Gutzmer, C. Wanhainen, Distribution of Sb minerals in the Cu and Zn flotation of Rockliden massive sulphide ore in north-central Sweden, Miner. Eng. 82 (2015) 125–135. doi:10.1016/j.mineng.2015.03.007.

[48] F. Habashi, E. Bauer, aqueous oxidation of elemental sulfur, 5 (1966) 469–471.

[49] J.E. Dutrizac, T.T. Chen, A mineralogical study of the jarosite phase formed during the autoclave leaching, Can. Metall. Q. 23 (1984) 147–157. doi:10.1179/cmq.1984.23.2.147.

[50] J.M.L. Kerbusch, The reaction between solid lead and chlorine gas, J. Solid State Chem. 9 (1974) 197–201.

[51] P. Schober, L.A. Schwarte, Correlation coefficients: Appropriate use and interpretation, Anesth. Analg. 126 (2018) 1763–1768. doi:10.1213/ANE.0000000000002864.

[52] A. Rabenau, The role of hydrothermal synthesis in preparative chemistry, Angew. Chemie - Int. Ed. 24 (1985) 1026–1040.

[53] F. Habashi, A new era in pressure hydrometallurgy, Metall. (2014) 27–34.

[54] J. Anwar, U. Shafique, Waheed-uz-Zaman, R. Rehman, M. Salman, A. Dar, J.M. Anzano, U. Ashraf, S. Ashraf, Microwave chemistry: Effect of ions on dielectric heating in microwave ovens, Arab. J. Chem. 8 (2015) 100–104. doi:10.1016/j.arabjc.2011.01.014.

668 [55] M. Omran, T. Fabritius, R. Mattila, Thermally assisted liberation of high phosphorus oolitic iron
669 ore: A comparison between microwave and conventional furnaces, Powder Technol. 269 (2014)
670 7–14. doi:10.1016/j.powtec.2014.08.073.
671 [56] S.W. Kingman, N.A. Rowson, Microwave treatment of minerals-a review, Miner. Eng. 11
672 (1998) 1081–1087. doi:10.1016/S0892-6875(98)00094-6.
673 [57] M. Al-Harahsheh, S. Kingman, S. Bradshaw, The reality of non-thermal effects in microwave
674 assisted leaching systems?, Hydrometallurgy. 84 (2006) 1–13.
675 doi:10.1016/j.hydromet.2006.03.056.
676 [58] L. Estel, M. Poux, N. Benamara, I. Polaert, Continuous flow-microwave reactor: Where are we?,
677 Chem. Eng. Process. - Process Intensif. 113 (2017) 56–64. doi:10.1016/j.cep.2016.09.022.
678 [59] OVAM, Decree of the Flemish Government adopting the Flemish Regulation on Sustainable
679 Management of Material Cycles and Waste Materials (VLAREMA), 2012.
680 [60] VLAREMA; ANNEX 2.3.2. CONDITIONS RELATING TO COMPOSITION FOR USE AS
681 BUILDING MATERIAL, (n.d.). https://navigator.emis.vito.be/mijn-navigator?woId=44707.
682

683